[CANCER RESEARCH 58, 5–13, January 1, 1998]

Advances in Brief

Etiological Involvement of Oncogenic Human Papillomavirus in Tonsillar Squamous Cell Carcinomas Lacking Retinoblastoma Cell Cycle Control[1]

Thomas Andl, Tomas Kahn, Andreas Pfuhl, Teodora Nicola, Ralf Erber, Christian Conradt, Wolfgang Klein, Matthias Helbig, Andreas Dietz, Hagen Weidauer, and Franz X. Bosch[2]

Molekularbiologisches Labor, Hals-Nasen-Ohren-Klinik [T. A., A. P., R. E., W. K., M. H., A. D., H. W., F. X. B.], Institut für Medizinische Biometrie [C. C.], Universität Heidelberg, Angewandte Tumor Virologie, Deutsches Krebsforschungszentrum [T. K., T. N.], 69120 Heidelberg, Germany

Abstract

Two hundred eight primary squamous cell carcinomas of the head and neck have been analyzed with respect to the presence of the retinoblastoma tumor suppressor protein, pRb. Of these, 23 tumors (11%) that preferentially localized to the tonsils revealed complete absence or dramatic reduction in the amount of pRb. Other cell cycle components, cyclin D1 and $p16^{INK4A}$, which are intimately related to pRb through an autoregulatory loop, were also dramatically decreased or overexpressed, respectively, in these pRb-defective tumors. On the other hand, the majority of the pRb-defective tumors contained the wild-type *p53* gene. No evidence was found for genetic defects at the *Rb* locus in these tumors. Very significantly, in 11 of 12 pRb-defective tonsillar tumors, but in none of 9 pRb-positive tonsillar tumors ($P < 10^{-7}$), DNA of oncogenic human papillomavirus types was identified, providing a strong indication for a human papillomavirus-associated etiology of these tumors and suggesting the functional inactivation of the pRb protein by the viral E7 gene product. In comparison to all head and neck squamous cell carcinomas studied, the pRb-defective tonsillar tumors were in general more poorly differentiated ($P = 0.0059$), and they were all metastatic at the time of resection. Of particular clinical interest, despite these adverse histopathological factors, the clinical outcome for these patients was relatively favorable, strongly implying that the pRb-defective tumors responded uniformly well toward postoperative radiation therapy.

Introduction

Although the vast majority of HNSCCs[3] arising in the western world shares common risk factors, *i.e.*, primarily tobacco and alcohol abuses followed by nutritional, environmental, and occupational exposures (1), these tumors show extensive diversity in biological and clinical behavior, including an unpredictable therapeutic response. The reason for this diversity is unknown but might, at least in part, be related to the functional inactivation of different sets of tumor suppressor genes in different tumors. In the multistep process of genetic changes underlying the development and progression of head and neck cancer, the only genetic factor known that is frequently inactivated by somatic mutations (in about one-half of the cases), is the *p53* gene (2).

The other classical and well-characterized tumor suppressor gene, the retinoblastoma susceptibility gene *Rb1*, is also functionally inactivated in various tumor types. The protein product of the *Rb1* gene, pRb, occupies a very central position in cell cycle control with intimate feedback interactions with the G_1 phase-specific cyclins D, E, and A, the cyclin-dependent kinases cdk2, cdk4, and cdk6, and the cyclin-dependent kinase inhibitors (most notably $p21^{CIP1/WAF1}$ and $p16^{INK4A}$ (3). In its underphosphorylated form, pRb prevents progression through the G_1 phase of the cell cycle. Upon phosphorylation, *e.g.*, by cyclin D1/cdk4, the E2F family of transcriptional activators is liberated from a protein complex centered around pRb, and E2F then promotes expression of several important S-phase genes (4). Opposing cyclin D1/cdk4, the cyclin kinase inhibitor $p16^{INK4A}$ negatively regulates the phosphorylation status of the Rb protein (5). Tumor cell lines lacking a functional pRb, from a wide variety of cell types, also do not express cyclin D1 (6) but overexpress $p16^{INK4A}$ (7), indicating the existence of an autoregulatory feedback loop between underphosporylated pRb, cyclin D1, and $p16^{INK4A}$. The impact of pRb defects on tumor growth has been demonstrated recently in transgenic mice that were either heterozygous for or which lacked the *p53* gene and that also harbored different SV40 T antigen constructs. Tumors induced by a T antigen fragment, unable to interfere with p53 function but inactivating pRb protein(s), developed slowly and displayed a high fraction of apoptotic tumor cells. On the other hand, fast tumor progression was observed when p53 was either inactivated by the complete T antigen or was absent (in p53−/−mice), and this was accompanied by a much lower rate of apoptosis (8).

Besides the T antigen of SV40 and the adenovirus E1A protein, the E7 protein of oncogenic HPVs (the most prevalent types in tumors are HPV 16 and 18) is also capable of functionally inactivating the pRb protein (9). In established cell lines, expression of oncogenic E7 results in reduced levels of cyclin D1 and elevated levels of p16 (10). The causal etiological association of HPV with cervical cancer is well established (11). However, whether pRb is consistently and completely inactivated in cervical cancer has not been determined.

HPV-DNA has also been found in HNSCC, but the reported incidence and the association with specific sites in the head and neck region has varied extensively (11). In more recent studies using PCR-based techniques, tonsillar carcinomas have emerged as a site with a consistently high incidence of HPV positivity (12–14). This is consistent with the fact that the tonsils, which posses an extensive surface area formed by a very large number of crypts, form a natural reservoir where microbial agents can accumulate and infect epithelial and lymphatic cells. HPV-positive HNSCC have been characterized only to a limited extent with regard to other molecular parameters. Again, variable and conflicting results have been reported. For instance, the incidence of p53 mutations was found to be inversely correlated with the presence of HPV (14), but p53 mutations were also reported to coexist with HPV (15).

A possible loss of pRb protein in HNSCCs has also been investigated. A low incidence of loss of pRb protein expression but a high

Received 9/3/97; accepted 11/19/97.

The costs of publication of this article were defrayed in part by the payment of page charges. This article must therefore be hereby marked *advertisement* in accordance with 18 U.S.C. Section 1734 solely to indicate this fact.

[1] The work was supported by grants from the Verein zur Förderung der Krebsforschung in Deutschland e.V. and the Tumorzentrum Heidelberg/Mannheim.

[2] To whom requests for reprints should be addressed, at Molekularbiologisches Labor, Universitaet-HNO-Klinik, Im Neuenheimer Feld 400, 69120 Heidelberg, Germany. Phone: 06221/566751; Fax: 06221/564604; E-mail: Franz_Bosch@krzmail.krz.uni-heidelberg.de.

[3] The abbreviations used are: HNSCC, head and neck squamous cell carcinoma; FISH, Fluorescence *in situ* hybridization; IHC, immunohistochemistry; LOH, loss of heterozygosity; HPV, human papillomavirus; ISH, *in situ* hybridization; RT-PCR, reverse transcription-PCR.

incidence of LOH at the *Rb* chromosomal locus 13q14.2 has been reported (16).

In this study, we have characterized a large number of HNSCCs for the presence of putative defects in the pRb regulatory pathway of cell cycle control and investigated a possible correlation with the HPV status, the p53 status, and with clinicopathological parameters.

Materials and Methods

Patient Materials. Biopsies of HNSCCs including adjacent mucosae, obtained after written consent from patients at the Ear, Nose, and Throat University Hospital, Heidelberg, were divided into two parts. One part was snap-frozen in precooled isopentane/liquid nitrogen immediately after surgery or tissue excision and stored at −80°C, the other part was formalin fixed and paraffin-embedded. Histopathological assessment on paraffin-embedded material was kindly performed by Dr. A. I. Born, Institute of Pathology, University of Heidelberg. The histopathological features of the tumors under study are summarized in Table 1. The treatment modalities for the patients with tonsillar carcinomas are presented in Table 4.

IHC. Frozen sections (6 μm thick) were fixed for 10 min in acetone at −20°C and air dried. Primary monoclonal antibodies or antisera were applied to the sections in PBS (pH 7.4). Staining was detected using the Vectastain ABC detection kit (Vector Laboratories, Burlingame, CA) following the instructions of the manufacturer. Paraffin sections were deparaffinized in xylene for 2 × 10 min and rehydrated with graded ethanol. Antigen retrieval on paraffin sections was performed by heating at 90°C for 15 min in 10 mM sodium citrate (pH 6.0). Endogenous peroxidase was blocked by incubating the sections in 3.5% hydrogen peroxide in PBS for 5 min. After blocking nonspecific reactivity for 1 h at room temperature with goat serum (Dianova, Hamburg, Germany), the sections were incubated with the primary antibodies at 4°C overnight (12 h) in the presence of 10% goat serum. For detection, biotinylated goat anti-mouse serum (Dianova) was added as secondary antibody for 30 min. After washing, the reagents of the Vectastain ABC kit were added. Staining was with diaminobenzidine (Vector Laboratories), and the sections were counterstained with methyl green (Sigma Biochemical Co., Deisenhofen, Germany). For immunohistochemical staining of $p16^{INK4A}$, only paraffin-embedded material was used.

Mabs. For pRb staining, clone 1F8 (Medac, Hamburg, Germany) was used on all sections. The antigen epitope for this antibody is not known. Those sections negative with 1F8 were also stained with clone G3–245 (PharMingen, San Diego, CA). This antibody recognizes an epitope located between amino acids 300–380 on the authentic human retinoblastoma protein. p53 was stained with Bp53-11 (Progen Biotechniques, Heidelberg, Germany), $p16^{INK4A}$ with rabbit anti-human $p16^{INK4A}$ polyclonal antiserum, and Ki-67 with MIB1 (both obtained from Dianova).

***In situ* Hybridization (ISH).** From plasmids containing cDNA inserts specific for cyclin D1 (17) and histone H3, cRNA probes were prepared by *in vitro* transcription and labeling with [^{35}S]-CTP. The probes were used for ISH as described before (18). Briefly, sections were fixed for 20 min at room temperature in 4% formaldehyde (freshly prepared from paraformaldehyde) buffered with 2× SSC. Pretreatment with proteinase K (0.2–0.5 μg/ml in 2× SSC, 0.1% SDS) was for 30 min at 37°C. The digestion was stopped with 0.1 M glycine/2× SSC, and the sections were postfixed for 5 min. After washing, an acetylation step was introduced to decrease background hybridization. Before ISH, sections were dehydrated. Hybridization took place overnight at 50°C and was followed by washing with 50% formamide, 2× SSC, a RNase A digestion, and a final wash with 50% formamide, 0.1× SSC. Sections were dehydrated again and dipped with Kodak photoemulsion.

FISH. The FISH analysis was performed basically as described in detail (19), but altogether a range of 10 centromeric DNA probes was used, specific for chromosomes 1, 7, 8, 9, 10, 11, 12, 15, 17, and 18. Two modifications of the procedure were introduced: (*a*) the cutoff value of cells appearing monosomic was determined for all DNA probes individually and was added to the disomic fraction; (*b*) a correction for the content of normal cells present to differing extent in all tumor biopsies was made to be able to better compare the aberrations in different tumor biopsies. Based on a mathematical formula, the smallest common disomic fraction of 200 cells after FISH with at least eight chromosomal probes to the same batch of cell suspension was taken as the maximal possible content of normal cells. After substraction of this normal disomic content, the remaining fraction was rescaled to 100%. In repeated experiments, the histological assessment has confirmed that this normal cell correction yielded very reliable estimates of tumor content. A detailed description of the modified FISH procedure will be presented elsewhere.[4]

Western Blotting. As described before (20), frozen material from approximately 50 cryosections (of 6-μm thickness) were collected in an Eppendorf tube, and 250 μl of SDS gel electrophoresis buffer were added. Samples were boiled for 5 min and loaded on a 13% SDS-PAGE. Proteins were transferred to polyvinylidene difluoride membranes (Immobilon, Millipore, Germany) by semidry blotting. For the detection of $p16^{INK4}$ protein, the same antiserum was used as for IHC.

RT-PCR Analysis. For the analysis of Rb mRNA, total RNA was extracted from selected biopsies that contained a very high proportion of tumor cells, exceeding 70% as judged from histological examination. The total RNA extraction kit (Qiagen, Hilden, Germany) was used. For reverse transcription, oligo-dT priming and the AMV RT enzyme (Promega Corp., Madison WI) were used. For second strand synthesis and amplification, primers Rb9 (5′-TATGAATTCTCTTGGACTTG-3′) and Rb17 (5′-TGTCAAGTTGCCTTCT-GCTTTG-3′), flanking the ends of exons 9 and 17, were added, and the reaction was allowed to proceed for 30 cycles. As controls, aliquots of the same cDNA preparations were used as template for at least two other amplification reactions, which routinely included E-cadherin and bcl-2. The latter showed highly variable protein expression levels in HNSCCs, and these correlated with the mRNA levels as analyzed by RT-PCR.[5] The resulting *Rb1*-specific PCR products were analyzed on agarose gels and showed the expected length of 737 bp.

PCR-Cycle Sequencing of Rb Exons 9–17 and p53 Exons 5–8. Details of the procedure for sequencing exons 5–8 of the *p53* gene have been described (20). Briefly, tumor DNA was prepared from microdissected tissues. PCR was performed using nested primers after initial amplification of a PCR fragment containing exons 5–8. Sequencing was performed using a DyeDeoxy Terminator Cycle sequencing kit (ABI-Perkin Elmer, Weiterstadt, Germany) on an ABI-Prism 310 Genetic Analyzer (ABI-Perkin Elmer, Weiterstadt, Germany). For further analysis of the Rb mRNA, the PCR products encompassing exons 9–17 (see above) were subjected to cycle sequencing in both directions, and the sequences were analyzed on the ABI-Prism 310 Genetic Analyzer.

Microsatellite Marker Analysis. The following microsatellite markers specific for chromosome 13 were analyzed: *D13S260, D13S155, D13S166, D13S153* (21), *D13S170, D13S217, D13S285,* and *D13S175* (linkage map set, panel 17; ABI Perkin Elmer). The PCR reactions were performed according to the protocols provided and analyzed on the ABI-Prism 310 Genetic Analyzer (ABI-Perkin Elmer). A reduction of the signal of one allele of 50% or greater was recorded as LOH. All tumor samples subjected to this analysis were histologically examined for the content of tumor cells, and only biopsies containing more than 60% of tumor cells were used without microdissection.

HPV-DNA Diagnosis by PCR. To ensure the presence of amplifiable DNA in tumor samples, DNA samples were tested with globin primers PC03 and PC04 (22). Samples with amplifiable DNA were then analyzed with anticontamination primers for the presence of HPV types 6, 11, 16, and 18 (23). Amplification reactions were performed using 200 ng of genomic DNA. Aliquots of the PCR products were electrophoresed through agarose gels and transferred to nylon membrane. The blots were hybridized with HPV type specific, [γ-^{32}P]dATP-labeled oligonucleotides in 5× SSC at 55°C. The filters were washed in 2× SSC, 0.1% SDS at 55°C and exposed to Kodak XAR films at −70°C with intensifier screens. Samples negative at this point were then tested using the HPV consensus primer system as described (24). Southern blots containing these PCR products were hybridized using consensus [γ-^{32}P]dATP-labeled oligonucleotides as described (24). Type identification of the consensus primer-positive DNAs was pursued using the cycle sequencing system from BRL. Positive and negative controls were included in each PCR run. The entire procedure was performed on coded DNA samples; the experimenters had no information as to the pRb status or any other clinical data.

Statistical Analysis. The Fisher's exact test and the χ^2 test were used for univariate analyses. The log rank test was used to evaluate Kaplan-Meier survival curves. For the comparison of DNA indices assessed by FISH with the

[4] A. Pfuhl and F. X. Bosch, manuscript in preparation.

[5] Unpublished results.

Table 1 *Clinicopathological features of the carcinomas*

Clinicopathology	No. of tumors
Site of primary tumor	
Tonsils	31
Oropharynx,[a] other sites	35
Larynx supraglottic	21
Larynx glottic	37
Oral cavity[b]	33
Hypopharynx	51
Nodal status	
N_0 (negative)	75
N_+ (positive)	133
Histological grading[c]	
G_1	21
G_2	108
G_3 and G_4	52
G_x	27

[a] Tonsils, soft palate, uvula, and base of tongue.
[b] Floor of mouth, hard palate, and tongue.
[c] In some cases, histological grading differed to some degree from the frozen material.

pRb status, the Mann-Whitney-Wilcoxon test was chosen. The statistical methods used are indicated in the tables. An initial significance level of $\alpha = 0.05$ was chosen. This α-level was adjusted for multiple testing ($n = 10$) by means of the Bonferroni procedure. The resulting significance level relevant for this study was $\alpha = 0.005$.

Results

pRb Protein Expression in HNSCC. pRb expression in frozen sections of 208 previously untreated HNSCCs (Table 1) was investigated by IHC. In 188 cases (89%), pRb staining was observed with a similar intensity as in normal squamous epithelium obtained from non-tumor patients (Fig. 1*a*). As to be expected, staining was strongest in actively proliferating cells, as indicated by parallel staining for the proliferation markers Ki-67 (by IHC with the MIB1 antibody or by ISH to the histone H3 mRNA, data not shown). In 23 (11%) of the HNSCCs analyzed, no pRb protein could be detected. As can be seen in Fig. 1*b*, only stromal and intratumoral lymphocytes stained positively, whereas the tumor cells were negative. The negative staining was confirmed in all cases in paraffin sections. In addition, the staining patterns were also confirmed using another pRb antibody (clone G3–245, not shown).

Anatomical Localization and Clinicopathological Features of pRb-defective HNSCC. As summarized in Table 2, the pRb-defective tumors occurred predominantly in the tonsils (65% *versus* 9% of the Rb-positive tumors; $P < 0.0001$; Fisher's exact test). Another two pRb-defective tumors were localized in the region of Waldeyer's ring, the remaining six were localized in the oral cavity and the larynx. Notably, none of the 51 tumors of the hypopharynx was pRb defective (Table 2). Twenty of 23 (87%) pRb-defective tumors (and 100% of the pRb-defective tonsillar carcinomas) had already metastasized to lymph nodes at the time of diagnosis. In comparison, 61% of Rb-positive HNSCCs had a positive lymph node status (N^+; $P = 0.015$; χ^2 test). The pRb-defective tumors were, in comparison with pRb-positive tumors in general, more poorly differentiated or undifferentiated ($P = 0.0059$; χ^2 test).

Expression of Cell Cycle-associated Proteins Cyclin D1, $p16^{INK4A}$, and p53. Because of the intimate feedback interactions between pRb and cyclin D1 and $p16^{INK4A}$, it was important to investigate the expression status of these latter components in pRb-positive and pRb-defective HNSCCs. Cyclin D1 expression was analyzed by ISH rather than by IHC, because in normal squamous mucosae, the level of cyclin D1 protein as seen by IHC was very low. In contrast, cyclin D1 mRNA could readily be detected by ISH. Fig. 1*d* shows a dark-field photomicrograph after ISH to the cyclin D1 mRNA of a consecutive section to Fig. 1*c*, which was pRb stained. Like pRb (Fig. 1*c*), cyclin D1 mRNA expression was positive in the tumor-adjacent nonmalignant cells but was markedly reduced in the tumorous area (Fig. 1*d*), although this area showed high proliferative activity, as measured by ISH to the histone H3 mRNA (Fig. 1*e*). Altogether, cyclin D1 mRNA expression was analyzed in 71 tumors, including 14 pRb-defective cases. All 14 pRb-defective but also 3 of the pRb-positive tumors showed reduced cyclin D1 mRNA expression (Table 3). None of the pRb-defective tumors showed overexpression of cyclin D1, which occurred in 17 (30%) of the pRb-positive tumors (data not shown). Thus, presumably as a result of negative feedback, reduced or absent cyclin D1 expression was strongly associated with defective pRb protein ($P < 0.0001$, Fisher's exact test; Table 3).

$p16^{INK4A}$ protein expression was examined by Western blot analysis and by IHC. In 54 of 62 tumors with positive IHC for pRb, the levels of $p16^{INK4A}$ protein were very low or undetectable. In contrast, 22 of 23 pRb-defective tumors markedly overexpressed $p16^{INK4A}$ (Table 3). Some examples are shown Fig. 2. Hence, in congruence with the inverse relationship reported previously between pRb and $p16^{INK4A}$ (7), $p16^{INK4A}$ overexpression was significantly associated with the absence of pRb protein ($P < 0.0001$, Fisher's exact test). In all cases examined by IHC, the results of the Western blots were fully confirmed (data not shown).

About 40% of HNSCCs including tonsillar carcinomas show overexpression of p53 in IHC. In contrast, only 4 of the 23 (17.4%) pRb-defective tumors showed overexpression of p53 by IHC ($P = 0.010$, χ^2 test; Table 3). None of the 15 pRb-defective tonsillar carcinomas overexpressed p53, resulting in an even stronger inverse correlation between defective pRb and p53 overexpression in these tumors ($P = 0.0005$, Fisher's exact test). In six pRb-defective tonsillar carcinomas, we have sequenced exons 5–8 of the *p53* gene. All six carcinomas showed wild-type p53 sequence (data not shown).

Lack of Correlation between pRb Defectiveness and the Genetic Status of the *Rb1* Alleles. It was of interest to examine whether the lack of pRb protein was due to genetic defects at the *Rb1* gene locus. The *Rb1* gene is located on chromosome 13q14. We studied the extent of allelic imbalances and/or LOH of eight microsatellite markers spanning the whole chromosome 13. Forty-four tumors were examined, of which 8 were pRb defective and 36 were pRb positive. One marker, *D13S153*, was directly located in the *Rb1* gene, for which 38 patients were informative. Of the eight pRb-defective tumors in this group, six did not show LOH at any marker, and two showed LOH at every informative marker (Table 3), suggesting an imbalance of the entire chromosome 13. In the pRb-positive group, there were more tumors with LOH at 13q14 than without LOH (Table 3). A similar pattern emerged after RFLP analysis (Table 3). At any rate, these data provide no evidence that LOH at 13q14 is associated with the expression pattern of the pRb protein ($P = 0.25$, Fisher's exact test). The data suggest that the lack of pRb protein is not accompanied with changes in the *Rb* gene but results from a different mechanism.

Rb1 mRNA Expression Appears Normal. We next sought to determine whether the absence of pRb protein in IHC (Fig. 1) was due to defects in *Rb1* gene expression. Semiquantitative RT-PCR analyses were performed on 8 selected cases of pRb-defective tumors with low stromal content and on 12 pRb-positive tumors. In addition, some biopsies of lymph node metastases were also available for analysis. In all pRb-defective cases, similar amounts of Rb1 mRNA could be amplified as from the pRb-positive tumors (whereas differential amounts of bcl-2 and E-cadherin sequences used as controls were amplified). The amplified sequences contained exons 9–17 of the *Rb1* gene, which partially encode the pocket region of pRb essential for protein function. These amplified products of 4 pRb-defective tumors were subjected to PCR cycle sequencing. No mutations could be detected in these exons (data not shown). These results indicate that

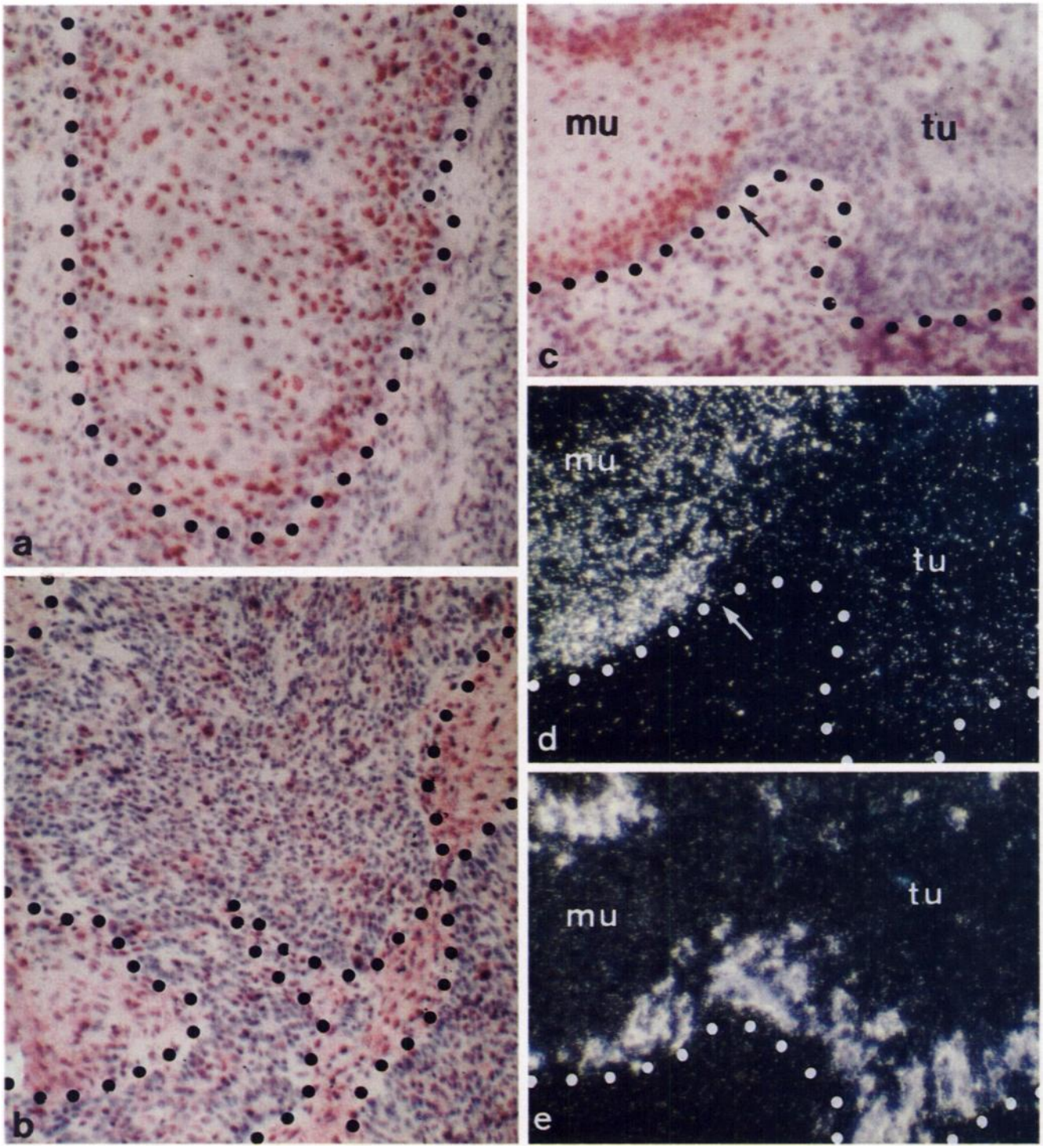

Fig. 1. pRb protein staining and comparison with cyclin D1 and histone H3 mRNA expression in tonsillar carcinomas. *a*, positive pRb staining; *b*, negative pRb staining in frozen sections of poorly differentiated tonsillar carcinomas. The *dots* follow the periphery of a tumor island. *c–e*, transition zone mucosa/carcinoma stained for pRb (*c*) and hybridized for cyclin D1 (*d*) and histone H3 (*e*) mRNA. The *dots* follow the mucosal and tumor periphery. The transition to tumor (*tu*) is marked by *arrows*. The tumor shows loss of pRb protein, whereas neighboring mucosa (*mu*) is still positive for pRb (*c*). The mRNA level of cyclin D1 was drastically reduced in the tumor (*tu*) compared to the neighboring mucosa (*mu*; *d*), whereas histone H3 mRNA expression and consequently proliferation was high in the tumor (*e*). *a* and *b*, ×240; *c–e*, ×400.

the observed absence of pRb was not due to defective mRNA expression and also not due to the production of aberrant proteins with mutations in exons 9–17.

Low Incidence of Numerical Chromosomal Aberrations in Rb-defective Carcinomas. Twelve pRb-defective and 25 pRb-positive carcinomas were analyzed by FISH by using centromeric DNA probes for chromosomes 1, 7, 8, 9, 10, 11, 12, 15, 17, and 18. Based on our previous study on HNSCC of all sites (19), the high-stage and high-grade pRb-defective tonsillar carcinomas should have revealed a high degree of aneuploidy and aneusomy. Strikingly, however, 11 of these turned out to be diploid or near-diploid, with few deviations to monosomy, trisomy, or tetrasomy. Examples of disomy and of aneusomy in some tumor cells are shown in Fig. 3. Incidentally, the 12th, aneuploid tumor has been presented in our previous study (see Fig. 1, *a* and *b* in Ref. 19). The observed difference in the aneuploidy rate between the pRb-defective carcinomas (n = 12; median DNA index

Table 2 *Correlation between pRb expression and clinicopathological parameters*

	pRb-defective	pRb-positive	*P*	Statistical test[a]
Tumor site				
Oral cavity	2	31		
Oropharynx	17	49		
Tonsil	15	16	<0.0001	Fisher's exact
Other	2	33		
Larynx	4	54		
Glottis	1	36		
Supraglottis	3	18		
Hypopharynx	0	51		
Nodal status				
N_0	3	72		
N_+	20	113	0.015	χ^2
Grading				
G_1/G_2	9	120		
G_3/G_4	11	41	0.0059	χ^2
G_x	3	24		
Smoking habit[b]				
Smokers	8	15		
Nonsmokers	7	0	0.0045	Fisher's exact

[a] See Table 3; for association of pRb-defectiveness with tumor site, tonsillar *versus* nontonsillar sites were compared. G_x tumors were not included in statistical analysis.
[b] Only patients with tonsillar carcinomas are included.

Table 3 *Characteristics of pRb-defective HNSCC and correlation with other molecular data*

	pRb-defective	pRb-positive	*P*	Statistical test[a]
p16 expression			<0.0001	Fisher's exact
Negative	1	54		
Overexpression	21	8		
Cyclin D1			<0.0001	Fisher's exact
Expression				
Reduced	14	3		
Normal	0	37		
Overexpression	0	17		
p53 expression			0.010	χ^2
Normal	19	98		
Overexpression	4	82		
HPV			<0.0001	Fisher's exact
Negative	1	9		
Positive	11	0		
LOH at 13q14[b]			0.25	Fisher's exact
Yes	2	19		
No	6	17		
Aneuploidy			0.0047	M-W-W
Median DNA index	1.055	1.300		

[a] M-W-W, Mann-Whitney-Wilcoxon test.
[b] *D13S153*, *D13S155*, and *XbaI* RFLP in intron 17 of *Rb1*.

from all centromeres analyzed, 1.055) and high-stage pRb-positive carcinomas (n = 25; median DNA index from all centromeres analyzed, 1.300) was highly significant (P = 0.0047; Mann-Whitney-Wilcoxon test; Table 3).

HPV-DNA in pRb-defective Tonsillar Carcinomas. Tonsillar carcinomas have been shown to be positive for HPV-DNA, although the reported incidence was variable (from 50–100%). Therefore, 21 primary tonsillar carcinomas (12 pRb-defective and 9 pRb-positive) plus 2 lymph node metastases (1 from a patient with a pRb-defective primary tumor) were studied for the presence of HPV-DNA. Using type-specific anticontamination primers (23), six pRb-negative tumors were positive for HPV16, whereas all tumors were negative for HPV types 6, 11, and 18. By performing consensus primer PCR (24), five additional HPV positives were detected, all of them pRb negative (Table 3). The PCR amplification products of three of these could be typed by means of cycle sequencing. One turned out to be HPV type 33 positive, and two were HPV type 16. In the latter two cases, which tested negative in the more sensitive type-specific PCR, this result suggests integration of the HPV-DNA with deletion of the HPV-E5 region in which the sequences corresponding to the type-specific primers are located. Examples of the Southern blot analyses for HPV-DNA are shown in Fig. 4. Of note, the two specimens 22 and 23 showing extremely strong HPV16 signals in the type-specific PCR (Fig. 4, *upper panel*) represent the primary tumor and a lymph node metastasis from the same patient, demonstrating the persistence of HPV16 in tumor progression in this case. Significantly, none of the pRb-positive tumors in this series showed the presence of any HPV type. The association of defective pRb with the presence of DNA of oncogenic papillomaviruses was extremely strong ($P < 10^{-7}$, Fisher's exact test), making a causal relationship and the viral etiology of these tumors most probable. It was interesting to note that the one pRb-defective carcinoma that was also negative for HPV (specimen 13, represented in both the *upper* and *lower panels* in Fig. 4) was the only highly aneuploid pRb-defective tumor detected by FISH. This tumor also was the one exception not overexpressing $p16^{INK4A}$.

Nonsmokers and pRb-defective Carcinomas. The analysis of the smoking history of the patients also revealed a difference to the patients with pRb-positive HNSCC, in further support of the papilloma viral etiology. The proportion of nonsmokers was higher among the patients affected with pRb-defective tumors than among those with pRb-positive tumors. This difference became significant when only tonsillar carcinomas were investigated (P = 0.0045, Fisher's exact test; Table 2).

Postoperative Patient Follow-up and Survival Analysis. The clinical outcome of 15 patients with pRb-defective tonsillar carcinomas (case group) and of 16 patients with pRb-positive tonsillar carcinomas has been followed; the mean follow-up times were 28 and 26.5 months, respectively. Because of the unfavorable features of the pRb-defective tumors, 12 patients received postoperative radiation therapy, 1 patient combined radiation/chemotherapy as postoperative treatment, and two others combined radiation/chemotherapy as primary treatment. In the control group, which included 5 cases without lymph node involvement, 10 patients received postoperative radiation, 3 received primary combined radiation/chemotherapy, and 1 received primary chemotherapy as sole treatment. Two patients in this group only received surgery (Table 4). The median disease-free survival time in the case group was 61.1 months *versus* 25.8 months in the control group. In the case group, two patients died *versus* 8 in the control group; these deaths were related to 1 *versus* 4 second primary tumors and 1 *versus* 4 local recurrences, respectively. These differences between the two groups were significant in both disease-free

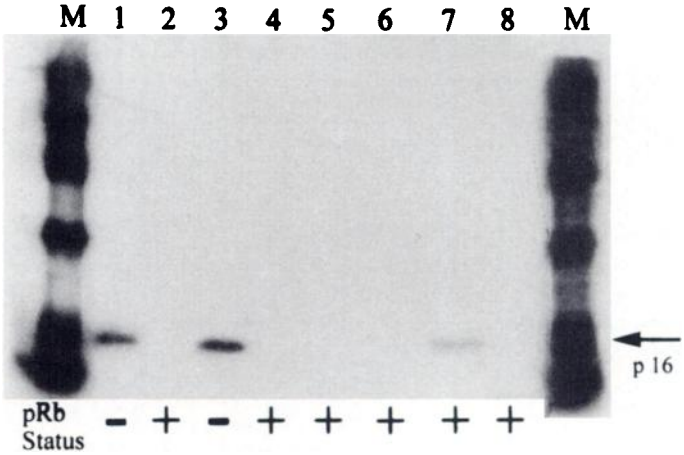

Fig. 2. Western blot analysis of $p16^{INK4A}$ in pRb-defective and pRb-positive HNSCC. Fifteen μg of protein extracted from different HNSCCs (*Lanes 1–8*; *M*, marker lanes) were analyzed. The filter was probed with the antiserum for $p16^{INK4A}$ (demarcated by an *arrow*). At the *bottom*, the pRb status is given: +, pRb-positive in IHC; −, pRb-negative in IHC. *Lanes 1* and *3*, pRb-defective tonsillar carcinomas; *Lanes 2* and *4*, pRb-positive tonsillar carcinomas; *Lane 5*, pRb-positive base of tongue tumor; *Lane 6*, hypopharynx tumor; *Lane 7*, floor of mouth tumor (both pRb- and p16-positive); *Lane 8*, supraglottic larynx tumor.

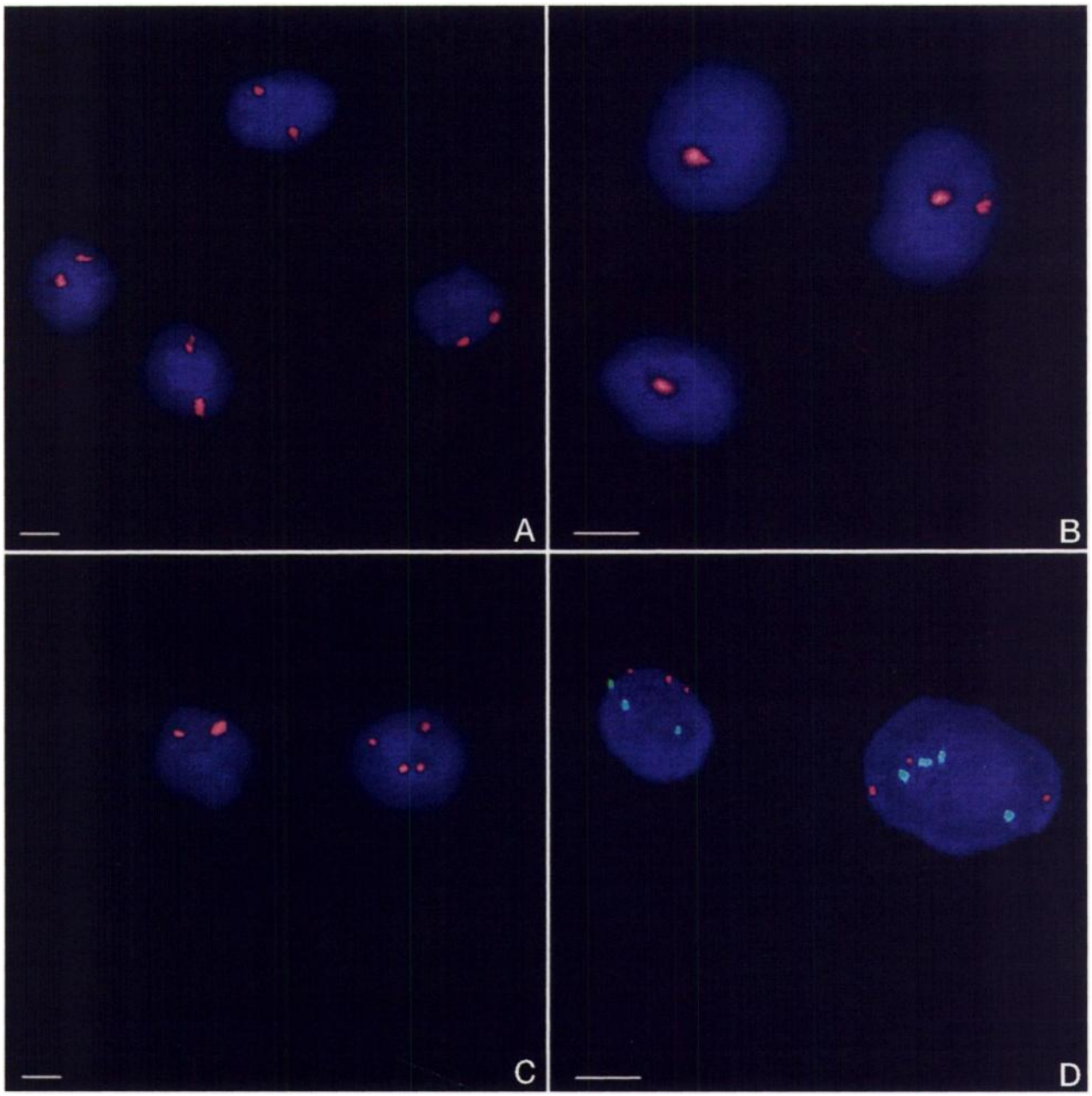

Fig. 3. Examples of limited numerical chromosomal aberrations in pRb-defective tonsillar carcinomas. Single-color FISH with the probe for chromosomes 11 (*A* and *B*) and 8 (*C*) and dual-color FISH with probes for chromosomes 8 (*red*) and 10 (*green*) (*D*) on single-cell suspensions. *A*, chromosome 11 disomic pRb-defective tumor cells; *B*, chromosome 11 disomic and monosomic tumor cells of another pRb-defective case; *C*, chromosome 8 disomic and tetrasomic pRb-defective tumor cells; *D*, chromosomes 8 and 10 trisomic and chromosome 8 trisomic/chromosome 10 tetrasomic pRb-positive tumor cells. *Bars*, 5 μm.

survival ($P = 0.028$, log rank test after stratification for staging) and overall survival ($P = 0.0071$, log rank test after stratification for staging). Fig. 5*a* (disease-free survival times) and Fig. 5*b* (overall survival times) show the Kaplan-Meyer curves generated from these data.

Discussion

In this report, we have for the first time provided several lines of evidence that oncogenic HPV types, most notably HPV16, are causally involved in the development of a distinct group of HNSCCs with several important features in common: (*a*) they lack pRb protein without apparent defects of the *Rb1* gene; (*b*) they fail to express cyclin D1 and aberrantly accumulate $p16^{INK4A}$; (*c*) they appear to retain wild-type p53; (*d*) they are poorly or undifferentiated, metastasizing stage IV tumors and preferentially occur in the tonsil and the region of Waldeyer's ring (tonsils, soft palate, base of tongue, and nasopharynx); (*e*) in contrast to the unfavorable histopathological features, they show significantly less chromosomal aneuploidy and aneusomy than high-stage HNSCCs in general; and (*f*) despite the very adverse histopathological features, but in line with the low degree of aneuploidy, the clinical outcome for the affected patients is relatively favorable. This latter finding indicates that the pRb-defective tumor cells respond uniformly well to radiation (and perhaps also to chemotherapy), resulting in a good disease control. Thus, although the therapeutic response of HNSCCs in general is unpredictable, the pRb-defective, HPV-positive tonsillar carcinomas appear to represent a distinct tumor entity in head and neck cancer, requiring uniform patient management.

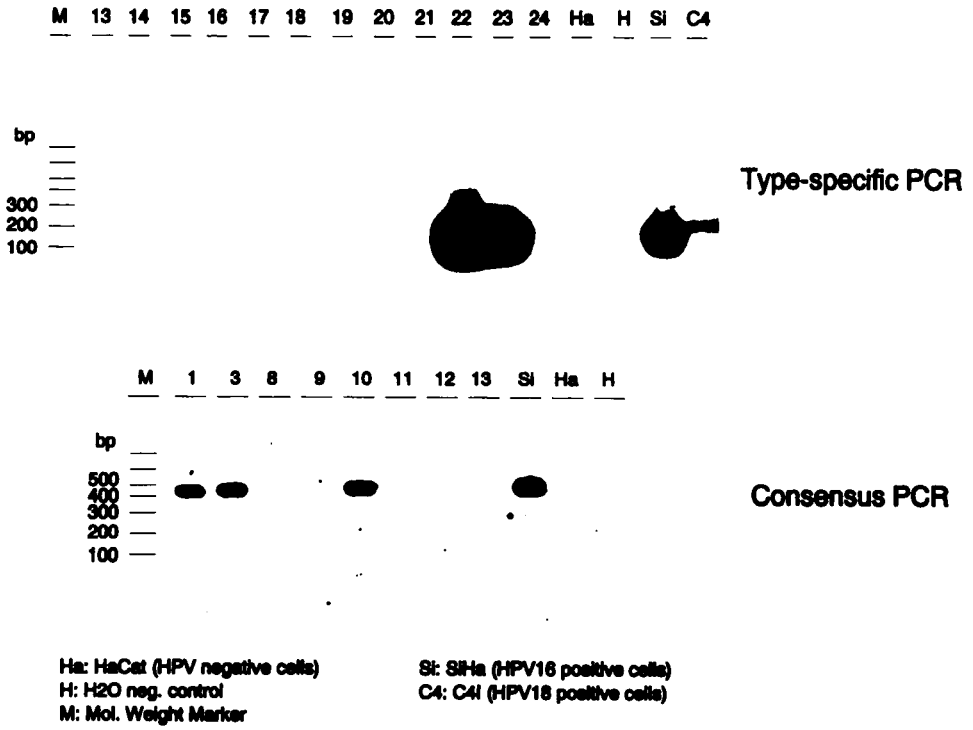

Fig. 4. Presence of oncogenic HPV-DNA in pRb-defective but not in pRb-positive tonsillar carcinomas. Southern blot analysis of the PCR products obtained after amplification of genomic DNA from tonsillar carcinomas as well as from HPV-positive and -negative cell lines with type-specific primers for HPV types 6, 11, 16, and 18 (*upper panel*) and consensus primers (*lower panel*). The amplified products were hybridized with radioactively labeled type-specific or consensus primer-specific oligonucleotide probes, respectively. The SiHa and C4-I cervical carcinoma derived cell lines used as controls contain HPV16 and HPV18-DNA, respectively, whereas the keratinocyte cell line HaCaT is HPV negative. Exposure to X-ray films was 2 days for the type-specific PCR and 5 days for the consensus primer PCR. For further details, see "Materials and Methods."

The examination of cyclin D1 and $p16^{INK4A}$ expression has provided strong support for the notion that the failure to detect the pRb protein in these tumors indeed reflected the functional inactivation of pRb and not merely epitope masking. It was puzzling that this functional inactivation of pRb was apparently not brought about by a genetic defect. There was no increased incidence of allelic loss of the *Rb1* locus at 13q14, and the partial mRNA analysis gave no hint of somatic mutations. Such a lack of association between loss of pRb protein and LOH at the *Rb1* gene locus has also been found in other studies on HNSCC (16). These studies and the results presented here indicate that the observed LOH on chromosome 13q14 in these tumor types is not related to genetic defects of *Rb1*.

The detection of DNA of oncogenic HPV types in these carcinomas has provided an explanation for the pRb-defective phenotype. The statistical analysis of the correlation between the presence of HPV-DNA and the pRb-defective phenotype (and the HPV persistence in the metastastic lesion) has made it most probable that HPV is causally involved, most likely due to the action of the E7 oncoprotein.

A possible viral contribution to tumor etiology has been discussed for a fraction of HNSCCs (reviewed in Ref. 11), but a causal relationship has not been demonstrated. In contrast to cervical cancer, where HPV-DNA can easily be detected in about 90% of the tumors and where extensive epidemiological studies have established oncogenic HPV types as causative agents, variable results have been published with respect to HPV infection in HNSCC. A preferential association of HPV with tonsillar carcinomas, including HPV-DNA integration and viral oncogene expression, was described in some of these studies (13, 14), but functional consequences were not analyzed.

Table 4 *Treatment modalities of 31 patients with tonsillar carcinomas*

For further details regarding pRb-defective and pRb-positive tumors, see text. Surgery was in two cases non-in sano; radiation consisted of 57–66 Gy over 6 weeks; chemotherapy consisted in four cases of two cycles of 70 mg of carboplatin/5FU per m^2, and in two cases, of 70 mg of cisplatin/5FU.

	Surgery	Postoperative radiation	Postoperative rad./chemo.[a]	Primary chemotherapy	Primary rad./chemo.
Yes	25	22	1	1	5
No	6	2	30	30	26

[a] rad./chemo., radiation/chemotherapy.

The concept that the disappearance of pRb from the HPV-positive tonsillar carcinomas is the primary event and that the concomitantly occurring aberrant expression of cyclin D1 (reduced) and p16 (accumulated) results from binding of the E7 protein to pRb is supported by studies of pRb-negative tumor cell lines and from transfection experiments. Reduced amounts of pRb have been shown in E7-expressing cell lines (Ref. 25 and references therein). In addition, expression of transfected pRb-binding viral oncogenes resulted in overexpression of p16 and reduced expression of cyclin D1 (26, 27), similar to the expression pattern in HPV-positive/pRb-negative tonsillar carcinomas observed in the present study. In a recent study, pulse/chase experiments have implicated a similar mechanism for pRb inactivation (28), as has been documented for p53 by E6, *i.e.*, degradation through the ubiquitin-proteasome pathway (29). Taken together, these results demonstrate that one of the primary targets of HPV in the course of the malignant conversion of squamous epithelial cells is the pRb protein, resulting in the disruption of the regulatory circuitry composed of pRb, cyclin D1, and p16.

The data presented raise the following important questions: (*a*) what could be the reason for the favorable response of the pRb-defective tumors toward postoperative radiation and/or chemotherapy; (*b*) why do these tumors not undergo an extensive genomic instability resulting in chromosomal aneuploidy and aneusomy, as observed in HNSCC in general; and (*c*) are these phenomena interconnected? The answer to these questions may well relate to the status of the *p53* gene in these HPV-positive, pRb-defective tonsillar carcinomas. None of the HPV-positive tonsillar carcinomas showed overexpression of p53, and the wild-type status of exons 5–8 was confirmed in six of these cases by PCR cycle sequencing. Mutations in the *p53* gene have been closely linked to an increased genomic instability of tumor cells and cancer-prone cells. p53 mutations have also been linked to increased resistance of tumor cells against various antitumor drugs and therapies (Ref. 30 and references therein). On the other hand, pRb-defective cultured cells and tumors are highly sensitive to apoptotic stimuli,

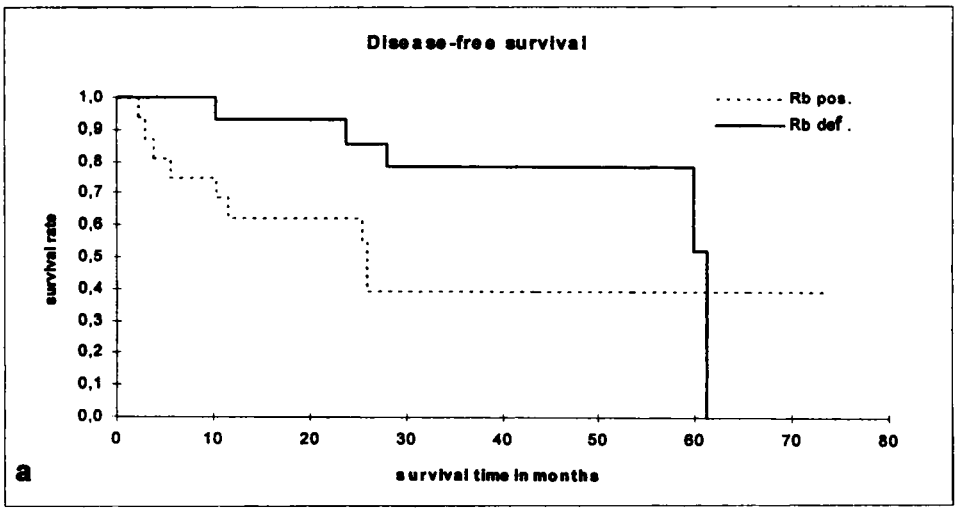

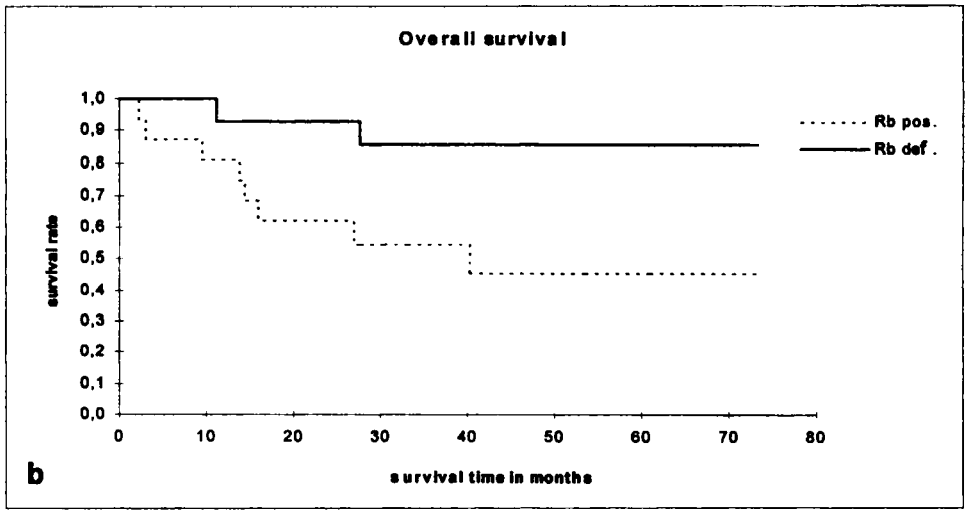

Fig. 5. Comparison of disease-free survival (*a*) and overall survival (*b*) between patients with pRb-defective and patients with pRb-positive tonsillar carcinomas. Kaplan-Meier curves are shown. The survival percentages are on the *y-axis*; the follow-up times in months are on the *x-axis*. In *a*, after stratification for tumor stages, the disease-free interval of patients with pRb-positive tonsillar carcinomas was significantly shorter as compared with those with pRb-defective tonsillar carcinomas ($P = 0.0019$, log rank test). Note that the abrupt ending of the curve in the case group was because of seven patients remaining disease free at the time of evaluation with a follow-up time marginally less than 61.1 months. In *b*, overall survival of the patients with pRb-positive tonsillar carcinomas was shorter than of those with pRb-defective tonsillar carcinomas ($P = 0.0071$ after stratification for tumor stages, log rank test).

despite the capacity to proliferate even under growth-limiting conditions (8, 31). Based on our observation of a largely retained diploid genotype of the HPV-positive, pRb-defective tonsillar carcinomas (and a highly aneuploid genotype of the exceptional HPV-negative case), it seems possible that the p53 protein in these tumors is not completely inactivated by the HPV-E6 protein. Although this is speculation at present, it is actually supported by recent observations of relevance. Although forced overexpression of the E6 protein directs p53 protein to proteolytic degradation (29) and results in inhibition of p53-mediated transactivation (32), the level of E6 in several cervical carcinoma cell lines was found to be insufficient to inhibit p53-mediated transcriptional activation. Thus, the presence of HPV E6 sequences does not appear to functionally correspond to mutations in the *p53* gene (33). Furthermore, these authors have shown that these cervical cell lines can exhibit intact cellular response mechanisms to genotoxic stresses such as those exerted by radiation and chemotherapeutic drugs (34). On the other hand, when E7 was transfected into primary human epithelial cells and the transfected cells were challenged by DNA damage, there was a bypass of the G1 growth arrest, despite elevated p53 protein levels (35). Such E7-transfected cells retain long-term genomic stability (36). These experiments show that there is an interconnection between pRb and p53 in which the functional inactivation of pRb by E7 is dominant over intact p53 in terms of the failure to arrest growth, but the "guardian" function of p53, including the capacity to induce apoptosis, appears to remain intact. In analogy to these important studies in cultured cells, we propose that p53 may still be functionally active in the HPV-positive, pRb-defective tonsillar carcinomas, preventing increased chromosomal aberrations and retaining a radiation- and chemotherapy-sensitive phenotype. This hypothesis needs to be tested in tonsillar carcinoma-derived cell lines harboring HPV.

Our findings may also be of clinical relevance for the pRb-defective HNSCCs from the other oropharyngeal sites as well as the larynx and oral cavity. We are presently investigating whether pRb-defective tumors from these sites are also causally related to HPV infections and, in particular, display a similar positive response toward postoperative radiation therapy. Furthermore, it should be interesting to examine HPV-positive cervical cancers for a possible relationship between pRb protein status and clinical outcome and, conversely, pRb-defective small cell and non-small cell lung cancers for a possible relationship between HPV and clinical outcome.

Acknowledgments

We are greatly indebted to Drs. H. Maier, C. Reisser, J. A. Tasman, and F. Wallner for collecting and processing the tissue specimens. We also thank A. Schuhmann, C. Enders, and C. Lohrey for technical support and S. Haas for $p16^{INK4A}$ immunostaining. We specifically thank Dr. A. I. Born, Institute of Pathology, University of Heidelberg, for histopathological assessment and helpful discussions and Dr. H. zur Hausen for his interest and support.